

CHAPTER SIXTY TWO

SHORT-CRESTED BREAKING WAVES

P.C. Machen¹

Abstract

The likely effects of short-crested (sc) breaking waves on ships and structures are summarised in the case of the simplest non-trivial sc sea at medium/high crossing angle. Typical experimental data of sc breaking wave-height and sc water particle speeds are given at model-scale.

1. INTRODUCTION

In recent years, more attention has been devoted to extreme waves (e.g. 15). It is suggested that there are at least two classes of extreme waves, which frequently may break:

- a) "Tail of the distribution" - type waves where two or more waves are temporarily superposed (16).
- b) Current-wave interaction, producing high steepness waves (14, 17, 26). To these should probably be added a third category:
- c) Short crested waves, in particular where high waves come together from two or more directions at middle or high crossing angle. An inshore example is given in Figure 1.1



Figure 1.1: Near-shore short-crested breaking wave formed from two obliquely-crossing waves.

Little attention has been paid to the last of these. Salter (23) formed a three-dimensional deep-water plunging wave by arranging that the phases of waves from an array of generators came into coincidence at a point. Halliwell and Machen (10) pointed out that short-crested (sc)

¹ Senior Research Associate, University of Newcastle upon Tyne, U.K.

breaking waves could be higher than long-crested and gave some results for shallow water. Hsu and Silvester (12) and Hsu (13) compared these results with predictions based on a third-order perturbation analysis.

The term 'short-crested' sea is often used to describe any sea having components from more than one direction, but in this paper the simplest non-trivial case will only be considered, that is a sc sea composed of two equi-amplitude equi-period waves crossing obliquely. It is to be expected that before breaking the finite-amplitude standing wave research reported in the 1950s and 1960s may be relevant. A step towards three-dimensional behaviour was made by Verma and Keller (28), and a third-order perturbation analysis of two obliquely-crossing waves was made by Hsu et al (11). Roberts (21) generalised and extended the analysis of the resonance behaviour of steady sc waves, using the preferred term "harmonic resonance".

In this paper, we begin in Section 2 by examining the loss of HMS COBRA in 1901 to which sc waves may have contributed. After some general discussion of sc breaking waves, some results are given in Section 3 from an experimental facility of two intersecting channels and sc steepness is compared with limiting long-crested steepness. The measurement of sc water-particle speed is considered in Section 4 where some success with a hot-film anemometer is reported.

2. THE IMPORTANCE OF SHORT-CRESTED BREAKING WAVES FOR SHIPS AND STRUCTURES

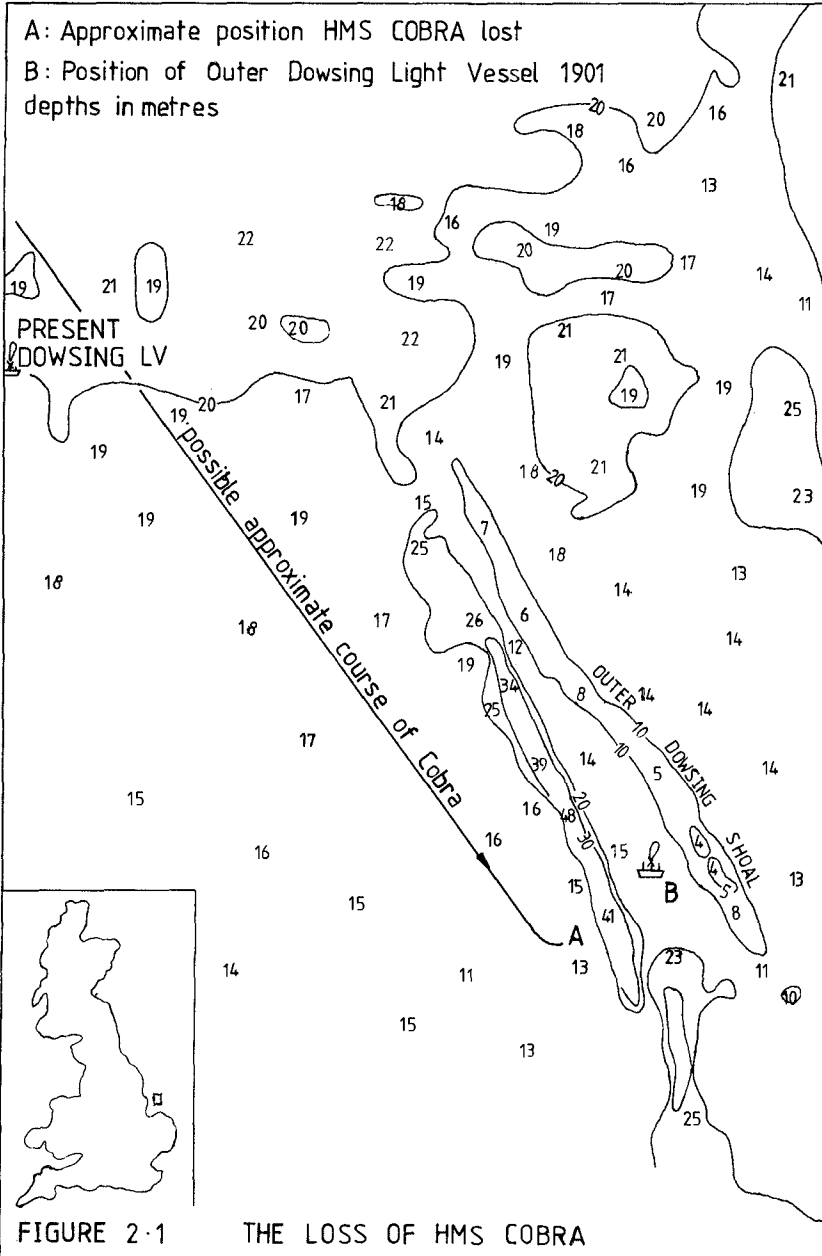
In a wind-sea, the angles between directional components are small and whitecapping will accord to normal criteria. The short-crestedness of the sea might be described as of low entropy. On the other hand, if we imagine two separate long-crested waves (associated perhaps with a swell or highly peaked spectrum) crossing obliquely at medium or high angle, then a high energy event with modified breaking criteria is possible.

In the case of such a crossing event the secondary wave flux can be produced by refraction around a shoal, by reflection from a deep-channel or structure, or by similar action through the action of a current regime. Clearly in these cases the secondary source is an image source. High crossing waves due to an image source are in practice likely to be rather localised.

Equally a secondary source could be real in the sense of wave flux from a second storm or from a wind-shift, but there is some experience that the short steep seas caused by very strong winds attenuate quite quickly when the wind drops or changes direction (see for instance Fig. 2 of (22), (6) and (8)); a secondary real wave flux is therefore only likely to be of the same order as a high primary source in a localised region of time and space.

2.1 Loss of HMS COBRA

Pierson (19) discussed the loss of two trawlers in the North Sea, suggesting that crossing waves could be to blame. Recently Faulkner et al (7) re-examined the loss of the torpedo-destroyer HMS COBRA in the North Sea in 1901 (their principal interest being in the structural aspects of the vessel). In the case of COBRA, more information is available



regarding the position of the ship than in Pierson's and there is eye-witness evidence that it was lost in a crossing sea. The mate of the light vessel 2nm ($3\frac{1}{2}$ Km) to the north-east reported winds NNW Force 6, the helmsman wind NW, and heavy rolling was experienced when heading slightly north of east. In spite of the sea being described by the light vessel mate as only "middling rough" the ship was seen to execute three terrific plunges with waves breaking over her forecandle and the ship broke in two. Survivors described the sea as "a heavy sea, a cross sea, not a regular sea, the wind one way and the tide another, as though there had been a change in the wind" (7).

There was some ambiguity about the exact position but the COBRA was near the Outer Dowsing Channel, the general alignment of which is NNW/SSE (Fig. 2.1). At this point the west bank of the channel is steep with chart depths of 15m and 40m top and bottom respectively, and its lie is $N16^{\circ}W$ over a 3Km length. Waves from the NW/NNW would have been obliquely incident on the discontinuity, and those of middle and higher period would have been reflected. A simple analysis by Snell's law indicates that, at the state of the tide at the time, waves from the NW would have been reflected for periods of 8 sec and more; from the NNW, of 5 sec and more. Faulkner et al (7) estimated the characteristic wave period as 7 sec.

A crossing-wave regime would have been set up near the discontinuity. 7-sec waves would have implied a depth-to-wavelength ratio of about 0.24, and the primary wave flux, the reflected secondary component(s) and any swell would have been approximately superimposed until a breaking limit were reached. There remains some doubts, however, whether the short-crested seas were breaking, what contribution additional swell made, what effect tidal currents had, and to what extent the present-day chart indicates the bathymetry of 1901.

2.2 Summary of Short-crested Breaking Effects

There are other examples of the importance of short-crested wave effects both offshore and inshore, but restrictions of space preclude inclusion here. The effects of sc (breaking) waves on ships and structures are as follows:

- a) The sc pyramidal or breaking waves may present a vessel or structure with a steeper than expected wave environment, which may exceed normal steepness criteria before reaching instability.
- b) Along the centre-line of the sc wave the wavelength is $L \sec \alpha$ (α being defined in Figure 3.1) and a ship steaming in that direction is more likely to be entirely in a trough immediately before the bow is struck by the three-dimensional crest. (In two dimensions, an abnormal length of trough has been advanced as an important factor in the casualties off the South African coast (17)).
- c) The sc wave profile speed may be high (higher by a factor of the order of $\sec \alpha$).
- d) At breaking a sc jet or inverted saucer of water may issue from the crest. Little information is available about maximum water-particle speeds, but behaviour is likely to depend partly upon d/L . Some results

are given in Section 4.

- e) Silvester (25) discussed the effects of crossing waves on sediment movement. Increased sediment transport can accompany crossing waves.
- f) There are likely to be consequences for fatigue calculations.

3. SC BREAKING WAVES - THEIR MODELLING AND HEIGHT

3.1 Modelling

Although it might be expected by symmetry and neglecting energy losses at the wall, that two obliquely-crossing waves would be analytically the same as one wave obliquely reflected from a straight vertical wall, if the wall is of finite length the diffracted wave must be included. High energy crossing events are likely to be localised and the diffracted wave may have to be included in some general sc breaking waves. There are, therefore, two alternative crossing-wave circumstances which can be modelled, one including the diffracted wave (Set-up A) and the other not (Set-up B).

The decision which to model will be significant as the diffracted wave may be important for a considerable distance (2). Clearly A can be modelled by reflecting waves from a straight vertical wall, or alternatively by bringing together waves from two intersecting channels. B could be modelled in a large basin with an array of wave generator elements with their phases set such that two obliquely-crossing waves were generated, but depending upon the scale a diffracted wave may still make a significant contribution. There are further possible modelling problems.

The basin at the University of Western Australia has some attractive features (25) and perhaps lies somewhere between A & B. For reasons of finance and the need for a local facility, an A-type basin was built at Newcastle (Figure 3.1), in which the angle α is variable. It is however not an ideal facility and suffers from the following deficiencies: diffraction of wave energy takes place into the adjacent channel which is then subject to reflection at the paddle; the test aperture is rather limited; and the channels, being of finite width, can support standing waves, in spite of cross-wave filters.

3.2 Short-crested Instability Criteria

As α is varied (theoretically) between 0° and 90° , the sc behaviour changes from being purely progressive to purely standing. In the general case, the two principal instability criteria, as summarised in (10) & (13) are:

a) Kinematic: $u_{max} > f(C_s)$ (3.1A)

b) Dynamic: $v_{max} > h(g)$ (3.1B)

Where u_{max} and v_{max} are maximum water particle speeds parallel to the basin centre-line and vertically upwards respectively, $f(C_s)$ is some function of short-crested celerity and $h(g)$ is a function of gravitational acceleration. Here the terms kinematic and dynamic are preferred as used by Hsu (13) after Dean (5).

Clearly when α is high, the dynamic condition is likely to dominate.

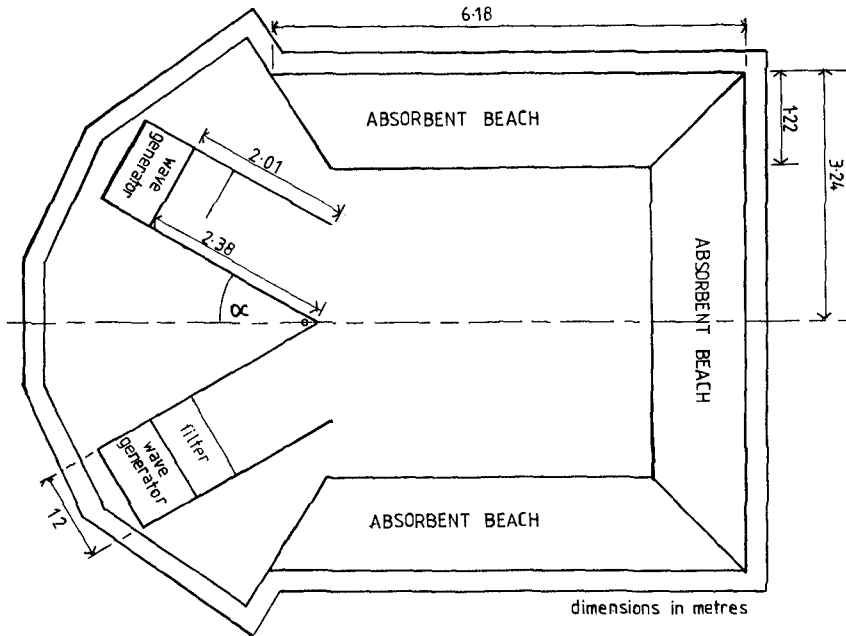


FIGURE 3.1 TWO-CHANNEL BASIN

Hsu (13) found a third-order solution to the dynamic stability criterion at all d/L from 0.05 to 0.5 for $70^\circ \leq \alpha \leq 90^\circ$. In the range $55^\circ < \alpha < 70^\circ$ he found the stability equation unsatisfied in a number of d/L values. On the other hand at lower values of α it may be expected that the kinematic condition will be dominant. In Equation (3.1A) $f(C_s)$ may be approximately equal to C_s , or alternatively a long-crested kinematic condition may be more appropriate. In this respect Hsu (13) found that for part-range of d/L a maximum value of u occurred which was less than C_s , finding it questionable that u_{\max} was a valid criterion for the highest wave where it was less than C_s .

The author has watched a large number of in-shore sc breaking waves and there appears to be a maximum value of α for a forward-breaking sc wave which is of the order of 45° . For wave-loading and slam considerations the kinematic condition is probably the more important criterion, but for ships experiencing pyramidal seas both conditions are likely to be of interest.

3.3 Short-crested wave height

In the model basin the sc breaking wave-height (H_{bs}) varied with the parent wave steepness ($K\bar{H}$), and there appeared to be a particular value of $K\bar{H}$ which gave the highest acceptable value of H_{bs} . At values of $K\bar{H}$

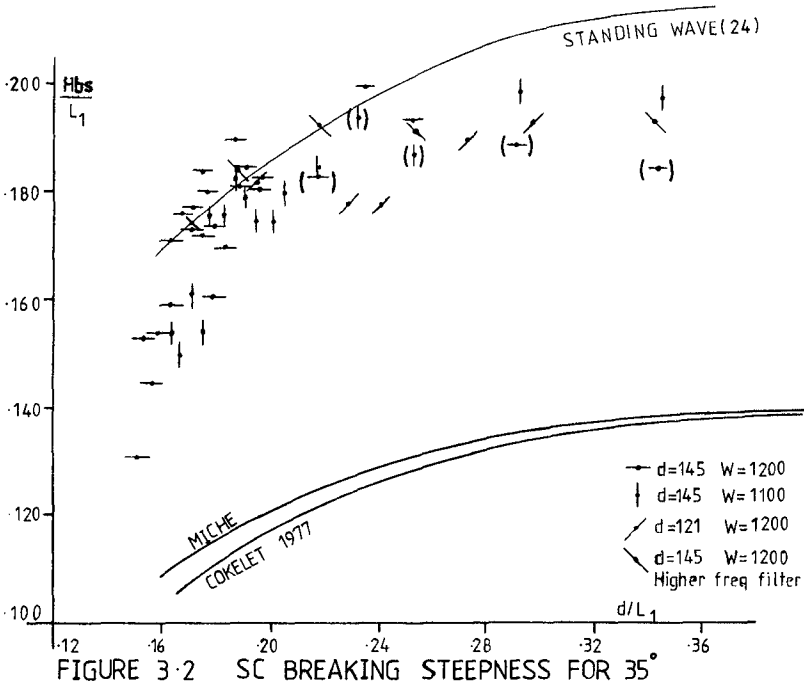


FIGURE 3-2 SC BREAKING STEEPNESS FOR 35°

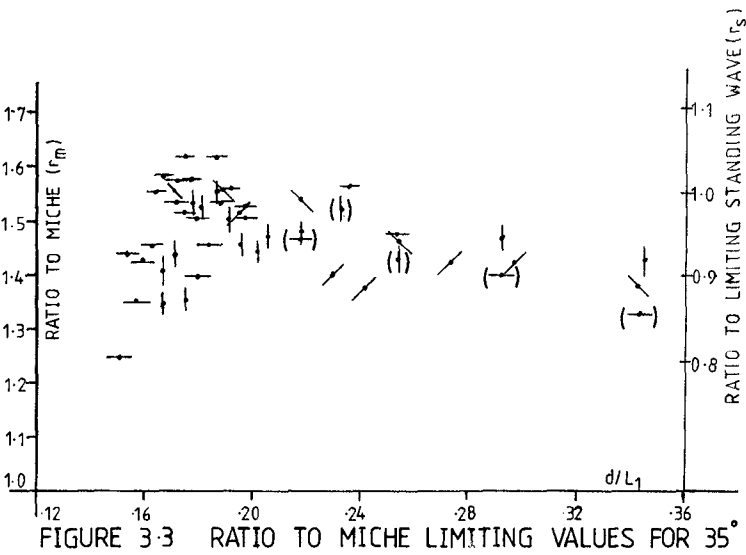


FIGURE 3-3 RATIO TO MICHE LIMITING VALUES FOR 35°

higher than the optimum, one of two circumstances applied, either H_{bs} decreased with the sc breaking wave being "pushed through" because of high energy concentration, or unacceptable spilling occurred in the channels. An envelope curve of H_{bs}/L_1 versus d/L_1 was plotted for $\alpha = 35^\circ$ (Figure 3.2); two values of channel width ($W = 1200$ & 1100mm) and two values of d (145 and 121mm) were used. The bracketted points are those where, at one d/L_1 , W was changed but the KH setting was not re-optimised. A series was also carried with a higher frequency cross-wave filter. The data is compared with limiting progressive steepness (according to Miche, and Cokelet (3)) and limiting standing wave steepness (24)). Fig. 3.3 shows the ratios of the experimental data points to the Miche value (r_m) and limiting standing wave (r_s):-

$$\left(\begin{array}{c} r_m \\ r_s \end{array} \right) = \left(\begin{array}{c} 1/0.142 \\ 1/0.22 \end{array} \right) \frac{H_{bs}}{L_1 \tanh Kd} \dots\dots\dots (3.2)$$

Compare Figure 3.3 with Roberts' conclusion that deep water sc waves could be up to 60% steeper than progressive waves (21).

Daemrich et al (4) found that for $\alpha = 20^\circ$ the height of a Mach Stem breaking wave did not exceed the predicted Miche limiting value for progressive waves. Further work needs to be done, but this may indicate the sensitivity of behaviour to variation of α in the range 20° - 30° (21 Fig. 4).

4. WATER PARTICLE SPEED MEASUREMENTS

4.1 Experimental Method

Available was a Thermo-Systems Inc. 1054 Constant Temperature Anemometer, with which conical hot-film probes (1231W) were used.

Breaking waves represent a hostile environment for hot-film anemometry. The problem of air entrainment was however likely to be less severe if measurements were made only up to the location where the front face of the sc waves became vertical.

Regarding the air-water interface, there have been conflicting views. Baldy et al (1) felt that the exploration, by fixed probes, of the air and water flows near the interface was "not generally feasible" and went on to use a wave-follower mounting. Wills (29) used a fixed hot-wire probe at the interface, but he was interested in the air flow above the surface. His discussion of the problems facing the experimenter at the air/water interface is illuminating. Van Dorn and Pazan (27) recognised that the frequency response of the equipment was sufficiently high for an equilibrium value to be measured within a small distance of the probe traversing from air to water (in their case 0.1mm).

To measure velocity on the water-side of the interface is easier than on the air-side. The reason for this is that if measurements are made on the airside a high overheat may be necessary to rapidly evaporate the water film and this degree of overheat may increase the rate of accretion of any contamination from the water-surface onto the sensing element.

In the two-channel basin a water-surface suction and filtering system was used to reduce contamination, but it was still likely to be a major

problem. It was decided to use a low value of overheat to reduce accretion, and the lowest value which would give adequate sensitivity to flow was used. 4% overheat was chosen. The usual heat balance equation is:

$$\frac{e_b^2 R}{(R + R_3)^2} = \left[A + B (\rho V)^{\frac{1}{n}} \right] (T_s - T_e) \dots\dots\dots (4.1)$$

where e_b is the bridge voltage, R the probe resistance, R_3 the resistance in the other bridge arm, ρ density, V speed, T_s the sensor operating temperature, T_e the water temperature and A, B constants. For good sensitivity to flow variation, a high T_s is required, that is high overheat. The choice of a low overheat of 4% necessitated close control of T_e to be maintained.

A simple test of the probe traversing the interface was conducted (at an overheat of 4%) at a constant speed in a towing tank. By means of a suitable mounting and a string and pulley, the probe was caused to traverse a number of times the water surface which had previously been

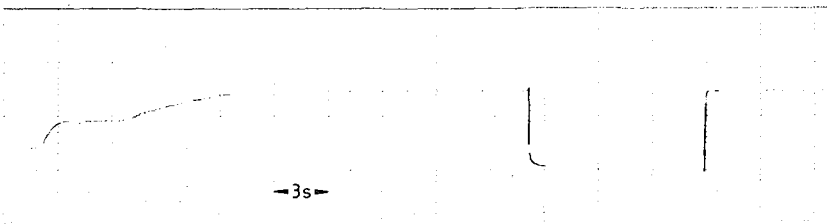


Fig. 4.1 Towing Tank Trial

swept clean, Figure 4.1 showing the bridge output voltage. The acceleration of the carriage to 1 m/s is clear, followed by traverses of the interface. The evaporation of the water film can just be seen. Upon successive immersion a consistent value of e_b was evident. The record was made on a heat recorder of bandwidth to about 50Hz which will therefore filter high frequency transients.

A calibration rig was constructed alongside the basin and water was drawn from the central area of the basin and discharged onto one of the absorbent beaches (Figure 4.2). The calibration rig had similarities to that used by Goodman and Sogin (9) who demonstrated that heat transfer was not affected by whether the flow was turbulent or laminar. In the calibration rig for the present work, Reynold's Numbers were in the range 1.5×10^4 to 4×10^4 . Temperature increase through the calibration rig was about 0.05°C which was equivalent to a change in speed of the order of 1%.

One would expect two principal reasons for changing calibration, dirt accumulation on the probe and temperature variation.

a) Dirt accumulation: Richardson and McQuivey (20) proposed that a dirty probe behaved as a clean probe at lower overheat, but Morrow and

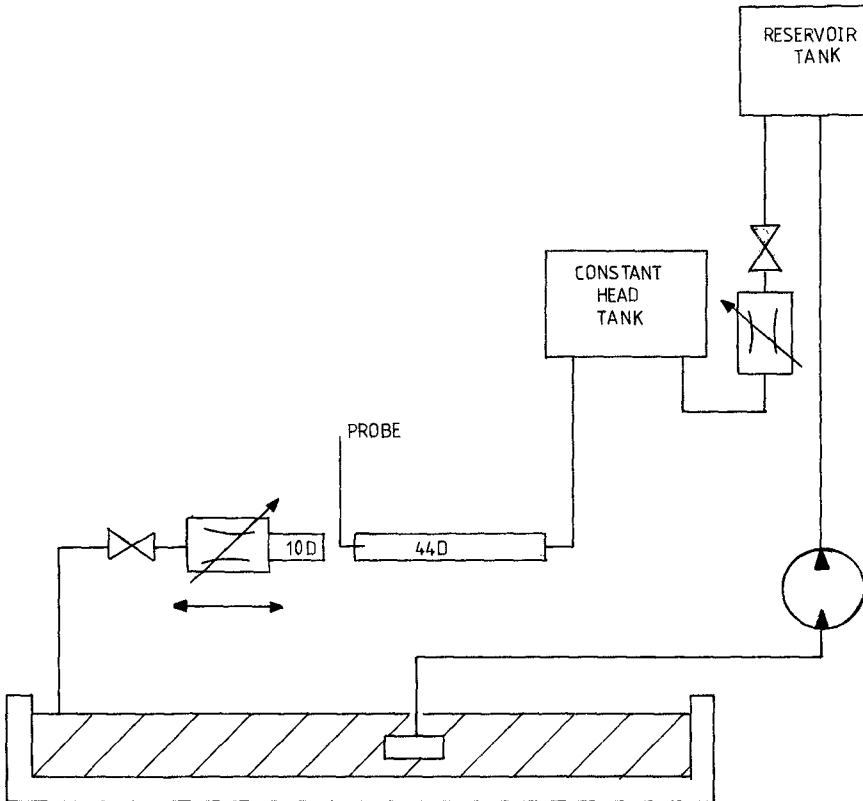


FIGURE 4-2 CALIBRATION RIG

Cline (18) concluded this was untrue. Because of the anticipated high drift from water surface contamination a second simple test was conducted with a highly contaminated water surface, at an overheat of 4%. The probe was mounted such that it was wetted by the crests of a series of waves. The output was monitored and it was noted that for the condition of the water at the time, rapid degradation occurred when the drying time between wave crests exceeded 0.7sec., but no degradation occurred for less than 0.6sec. This drift was probably due to the progressive accretion of water surface contamination onto the probe. Therefore for subsequent measurements small wave periods were chosen and the probe calibration was re-checked and the probe cleaned after every measurement.

b) Temperature variation: One standard method of allowing for a change of T_e by varying overheat slightly for the same e_{b0} was unsatisfactory in this case for the degree of control required. It can be easily shown from Equation (4.1) that for the same probe setting and the same flow one would

expect an approximately linear relationship between e_b^2 and e_{bo}^2 . Experimental confirmation is given in Figure 4.3 where the middle group of points relates to small changes in T_e and the low and high values are a result of dropping and raising overheat slightly, that is varying T_s . This linear relationship was used to correct measured values of e_b^2 to a base

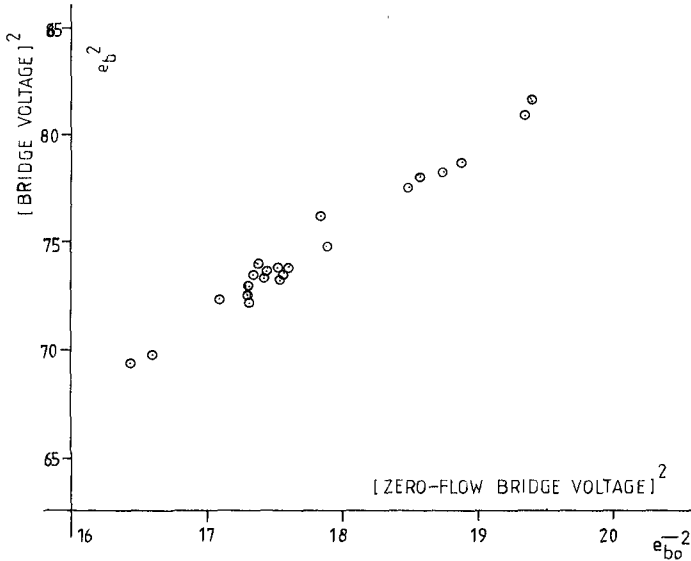


FIGURE 4.3 VARIATION OF e_b^2 WITH e_{bo}^2 FOR CONSTANT FLOW

value of e_{bo}^2 the square mean zero-flow measurement before and after calibration. The procedure also corrected for variations in other resistances. In Table 4.1 Runs 1 and 2 were calibration runs for a cleaned probe at differing water temperatures with similar values of e_b^2 after correction. For comparison Run 3 shows the calibration run for a lightly contaminated probe. The base value of e_{bo}^2 was 17.56.

Calib- ration run	T_e	e_{bo} BEFORE	CAL e_b	e_{bo} AFTER	e_{bo}^2	Correct- ion Factor	Uncorr- ected e_b^2	Correc- ted e_b^2	Remarks
1	18.3	4.16	8.455	4.16	17.26	1.017	71.45	72.56	Uncontam.
2	17.45	4.24	8.64	4.25	18.02	0.974	74.65	72.71	Uncontam.
3	17.5	4.25	8.49	4.25	18.06	0.972	72.08	70.06	Light Con- tamination

TABLE 4.1: Effect of Temperature Variation and Contamination

4.2 Results

Profiles of maximum total water particle speed U/C_1 were measured along the basin centre-line (average of 5 consecutive waves), with the right-angled probe pointing towards the channel apex. Figures 4.4a and b show the development of the U/C_1 profile (shown by the circled points) for $d/L_1 = 0.34$ at four distances from the apex (X/L_1). The corresponding sc L_1 wave profiles are also shown. For comparison the horizontal speed profiles (u/C_1) in a hypothetical long-crested wave of this height according to Van Dorn's hyperbolic equation is shown (27):

$$\frac{u}{C} = \frac{a}{b} \frac{z^1}{1-z^1} + \frac{u_0}{C}$$

Where z^1 is the fractional ordinate from trough to crest at which u is given, a & b are arbitrary constants 0.10 and 1.125 respectively. $u_0/C = 0.20$ and C is the wave celerity.

In Figures 4.5 to 4.7, U/C_1 profiles are shown at breaking for $d/L_1 = 0.29$, 0.24 and 0.19. Differing values of d and W were used. It is seen that there is good consistency of the U/C_1 profiles at breaking of the four values of d/L_1 . Measurement accuracy is estimated as $\pm 15\%$.

Table 4.2 summarises the maximum values of $U(U_{max})$ found for each d/L_1 , and compares it with linear pattern speed ($\sec \alpha$) and with a measured estimate of sc celerity C_s . It will be seen that maximum water particle speeds were less than pattern speeds except for $d/L_1 = 0.24$ for which there was variation in the sc jet speed; at these values of d/L this is qualitatively not in disagreement with Figure 4 of (13). However higher speeds later in the breaking process cannot be ruled out.

Further work is desirable on the crest values of U as breaking develops: measurements are required at lower d/L_1 values; and an increase of scale is desirable.

d/L_1	$\sec \alpha$	Measured C_s/C_1	Measured U_{max}/C_1
0.34	1.22	1.33	0.83
0.29	1.22	1.31	0.89
0.24	1.22	1.31	0.82-1.28
0.19	1.22	1.39	0.78

Table 4.2 Summary of U_{max}

Acknowledgement

The work is funded by the UK Science and Engineering Research Council through its Marine Technology programme.

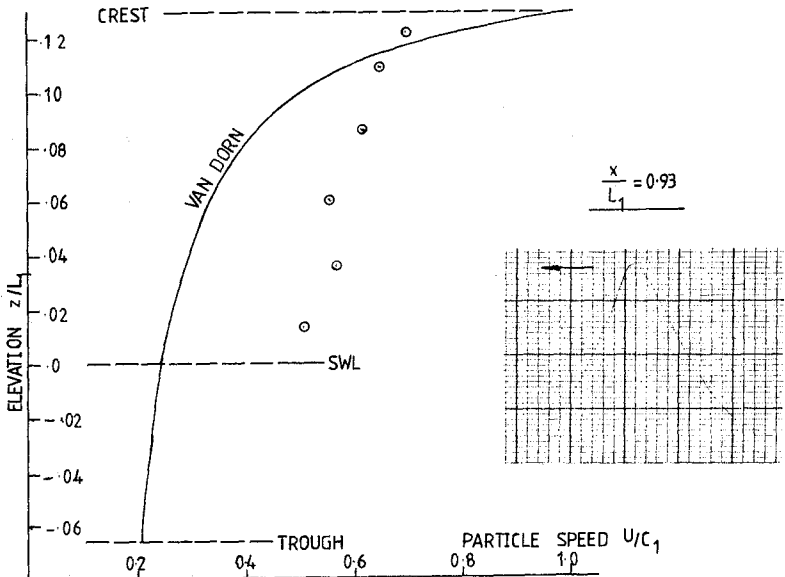
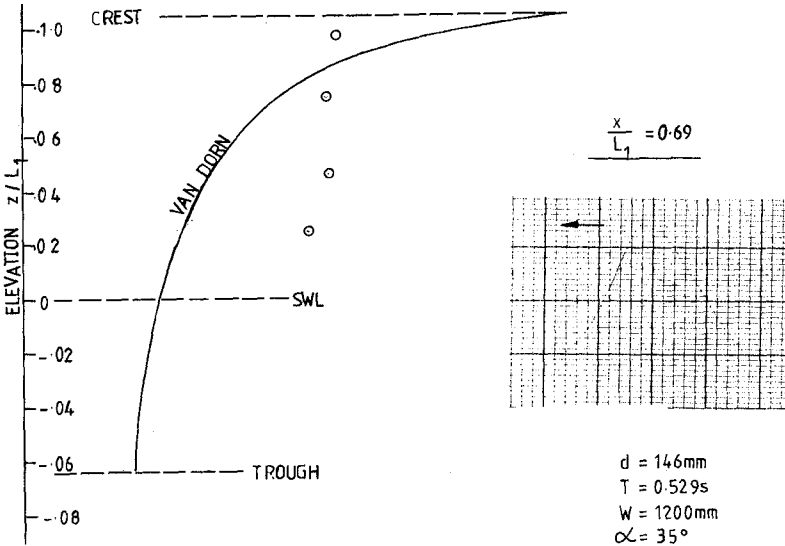


FIGURE 4-4a DEVELOPMENT OF SC WATER PARTICLE SPEED PROFILE ALONG CENTRE-LINE $d/L_1 = 0.34$

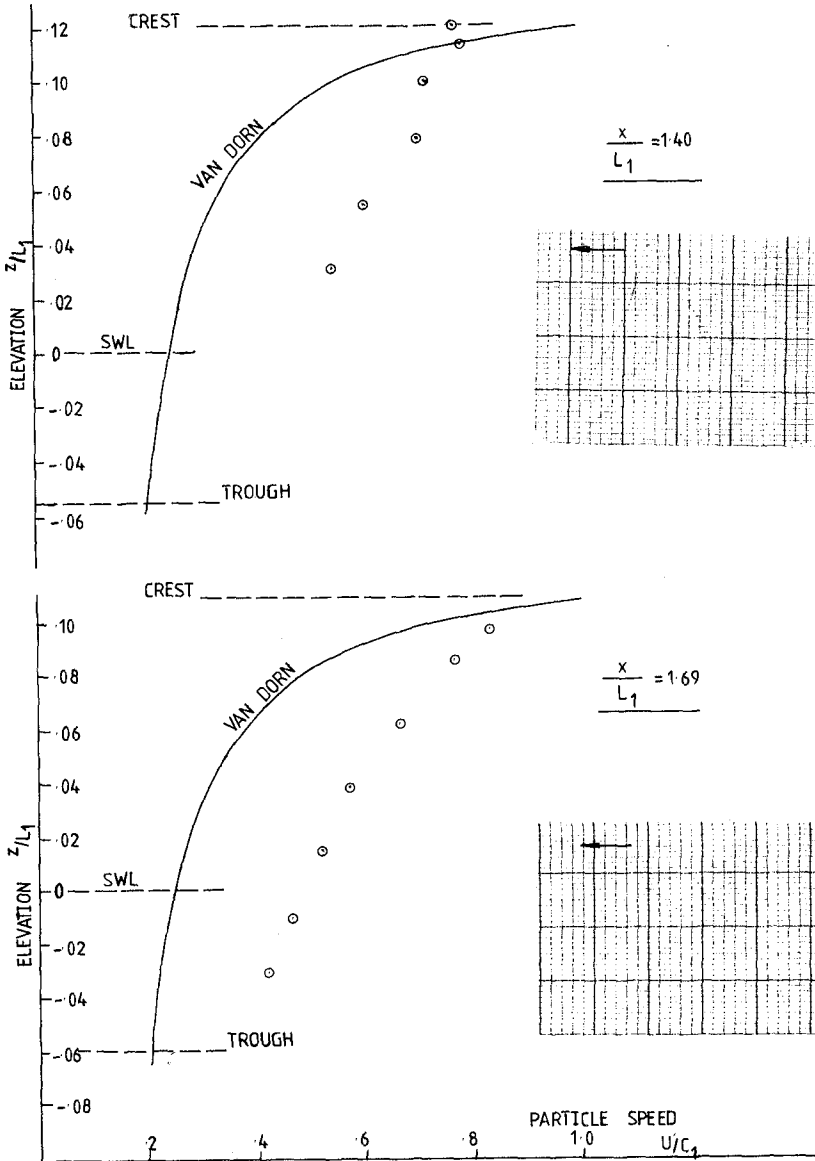
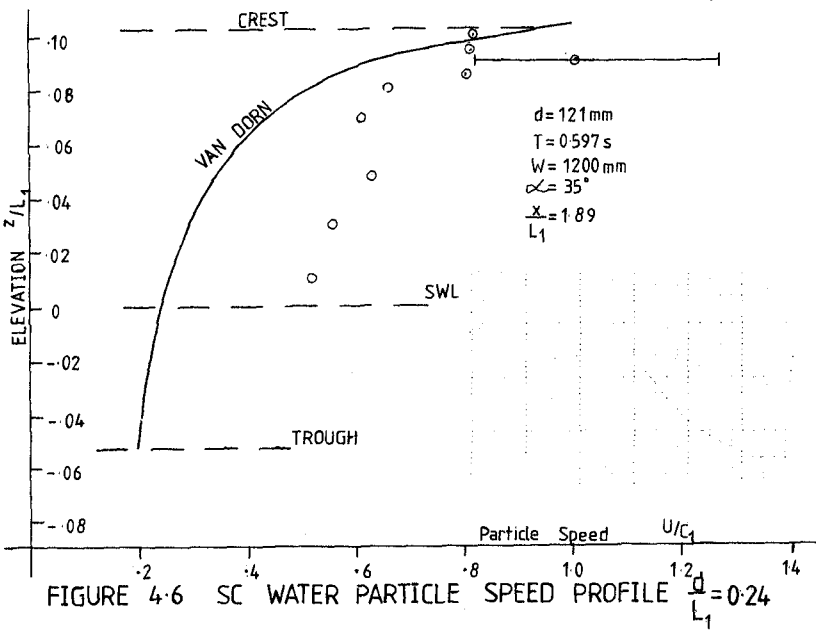
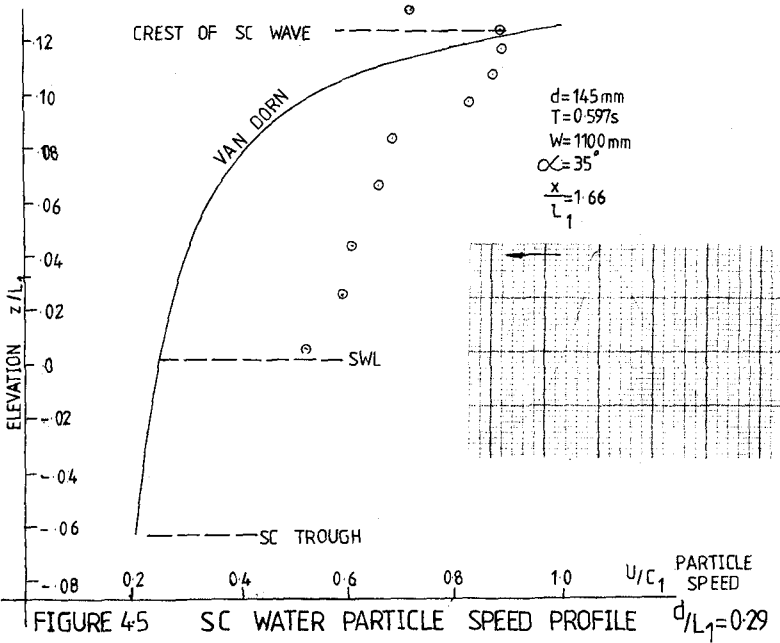
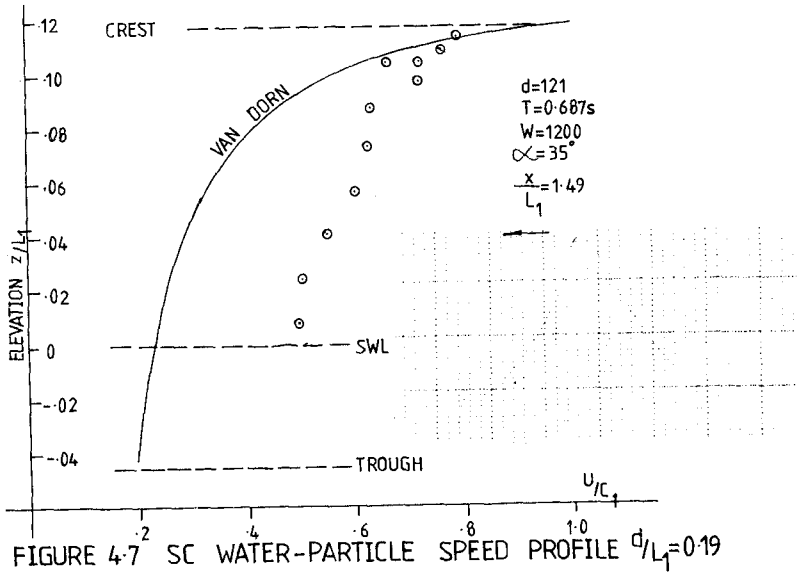


FIGURE 4.4b DEVELOPMENT OF SC WATER PARTICLE SPEED PROFILE ALONG CENTRE-LINE





REFERENCES

1. BALOY, S. et al (1978). Description of characteristics of a wave follower system for energy exchange studies on the vicinity of an air water interface. *Rev. Sci Instrum.* 49(8).
2. BERGER, U & KOHLHASE, S (1976). Mach-reflection as a diffraction problem. *Proc. 15th Coast Eng. Conf.* 1, 796-814.
3. COKELET, E.D. (1977). Steep gravity waves in water of arbitrary uniform depth, *Phil Trans Roy Soc. Lond.* A.286, 183-230.
4. DAEMRICH, K-F. et al (1983). Investigation of Mach-reflection including breaking and irregular waves. *Conf. Coast and Port Eng. in Dev. Count.*
5. DEAN, R.G. (1968). Breaking wave criteria: a study employing a numerical wave theory. *Proc. 11th Coast. Eng. Conf.*, 108-123.
6. EARLE, M.D. (1975). Extreme wave conditions during Hurricane Camille. *JGR* 80.
7. FAULKNER, J.A. et al (1984). The loss of HMS COBRA - a reassessment. *RINA Spring Meeting 1984*.
8. GERRITSMAN, J. & BEUKELMAN, W. (1980). Seakeeping trials with HNLMS TYDEMAN. Report 494 Delft Univ. of Tech.
9. GOODMAN, C.H. & SOGIN, H.H. (1974). Calibration of a hot-film anemometer in water over veloc. range 0.5 to 200 cm/s. In *Flow - its Measure & Control in Sci and Ind.*, 1 Pt.2.
10. HALLIWELL, A.R. & MACHEN, P.C. (1981). Short-crested breaking waves in water of limited depth. *Proc. Instn. Civ. Engr. Part 2.*, 71, 663-674.

11. HSU, J. (1979). 3rd order approximation to short-crested waves, *JFM* 90, 179-196.
12. HSU, J & SILVESTER, R. (1982). Discussion on Halliwell and Machen (1981). *Proc. Instn. Civ. Engrs. Part 2*, 73, 489-491.
13. HSU, J. (1983) On the limiting conditions for short-crested waves. *Conf. Coastal and Ocean Eng., Gold Coast*, 13-15 Jul.
14. KJELOSEN, S.P. & MYRHAUG, D. (1979). Breaking waves in deep water and resulting wave forces, *Proc. OTC*, Paper OTC 3646.
15. KJELSDEN, S.P. (1982). 2- & 3- dimensional deterministic freak waves, *Proc. 18th Coast. Eng. Conf*, 1, 677-694.
16. LONGUET-HIGGINS, M.S. (1974). Breaking waves - in deep or shallow water. *Proc. 10th Symp. Nav. Hydrodyn. Office Nav.Res*, 24-28 Jun 74.
17. MALLORY, J.K. (1975). Abnormal waves off the S. African coast - a danger to shipping. *The Nav. Arch.* 5, 82-84.
18. MORROW, T.B. & KLINE, S.J. (1974). The performance of hot-wire and hot film anemometers used in water, In *Flow - its Measurement and Control in Sci & Ind.* 1, 555-562.
19. PIERSON, W.J. (1972). The loss of two British trawlers, a study in wave refraction, *J. Nav.*, 25, 291-304.
20. RICHARDSON, E.V. & McQUIVEY, R.S. (1968). Measurement of turbulence in water. *Proc. ASCE*, HY94, 411-430.
21. ROBERTS, A.J. (1983), Highly nonlinear short-crested water waves. *J. Fluid Mech*, 135, 301-321.
22. SAETRE, H.J. (1975) On high wave conditions in the northern North Sea. *Proc. Oceanology International*, 280-289.
23. SALTER, S.H. (1978). The development of the duck concept. *Proc. Wave Energy Conf. London*, 22 Nov. 78.
24. SILVESTER, R. (1974). *Coastal Engineering*, 1, Elsevier.
25. SILVESTER, R. (1977). The role of wave reflection in coastal processes. *Proc. Coastal Sediments 77*, 639-654.
26. SMITH, R. (1976) Giant waves, *J. Fluid Mech.*, 77, 417-431.
27. VAN DORN, W.G., PAZAN, S. (1975): Laboratory investigation of wave breaking Part 2, deep water waves. *Scripps*, SIO 75-21.
28. VERMA, G.R. & KELLER, J.B. (1962). 3-dimensional standing surface waves of finite amplitude. *Phys. Fluids* 5, 52-56.
29. WILLS, J.A.B. (1976). A submerging hot wire for flow measurements over waves. *OISA Info* 20, 31-34.